

# Geophysical Research Letters

## RESEARCH LETTER

10.1029/2020GL090732

### Key Points:

- A regional atmosphere–ocean-coupled model is used to assess the influence of ocean tides on the atmosphere
- In summer, when tides cool sea-surface temperature, we find the mean air temperature and accumulated precipitation over land are decreased
- Smaller, but opposite, impacts of tides on British weather are found in winter

### Correspondence to:

A. K. Arnold,  
[alex.arnold@metoffice.gov.uk](mailto:alex.arnold@metoffice.gov.uk)

### Citation:

Arnold, A. K., Lewis, H. W., Hyder, P., Siddorn, J., & O'Dea, E. (2021). The sensitivity of British weather to ocean tides. *Geophysical Research Letters*, 48, e2020GL090732. <https://doi.org/10.1029/2020GL090732>

Received 16 SEP 2020

Accepted 19 DEC 2020

## The Sensitivity of British Weather to Ocean Tides

Alex K. Arnold<sup>1</sup> , Huw W. Lewis<sup>1</sup> , Patrick Hyder<sup>1</sup> , John Siddorn<sup>1</sup> , and Enda O'Dea<sup>1</sup> 

<sup>1</sup>Met Office, Exeter, UK

**Abstract** Tides in shelf seas greatly impact ocean mixing and temperature structure. Using a regional-coupled ocean–atmosphere prediction system, at ocean coastal process and atmosphere convection permitting scales, we assess the influence of tides on British weather by comparing simulations with and without tides. In summer, when seasonal stratification is particularly sensitive to tides, the sea-surface temperature is up to 6 K cooler in simulations with tidal mixing. Tides cool the air temperature over the sea by up to 3 K, and nearby land by up to 1.4 K. The mean air temperature across Great Britain land areas cools by 0.3 K with tides. Changes in near-surface stability result in decreases in summer mean wind speeds over the ocean. A 6% reduction in summer precipitation is found with tides, consistent with cooler temperatures. This study has implications for climate projections since global-coupled models typically do not include tides.

**Plain Language Summary** Ocean tides affect how heat is mixed through the shallow waters around the UK, which can affect the ocean surface temperature. We have used a new simulation approach which directly links detailed atmosphere and ocean models, to assess how the tidal influence on ocean temperatures affects the overlying atmosphere and the weather that develops further afield over land. We find tides have a stronger influence on the weather in summer than winter, and without tides around the UK, in summer, the average temperature would be warmer.

### 1. Introduction

Tidal mixing dominates the seasonal evolution of stratification in shallow seas, such as the North West European Shelf (NWS) region surrounding Great Britain (GB) (e.g., Bowers & Roberts, 2019; Simpson et al., 1978).

In winter, the shelf seas are well mixed through a combination of destabilizing surface cooling, strong wind forcing, and tidal mixing. In summer, strong surface heating and reduced winds tend to produce a stratified ocean vertical temperature structure (e.g., Elliott & Clarke, 1991), except in sufficiently shallow and tidally energetic regions such as the southern North Sea (e.g., Nauw et al., 2015; van Leeuwen et al., 1995) and Irish Sea (e.g., Simpson & Hunter, 1974) where tidal mixing dominates and the ocean remains well mixed throughout the year.

Timko et al. (2019) illustrated the importance of explicitly representing tides to improve the prediction of seasonal sea-surface temperatures (SSTs) in global-scale uncoupled ocean simulations, with SST cooling of about 1 K evident in many near-coastal regions. In general, tides and other near-coastal processes including wetting and drying and regions of freshwater influence are not currently well represented in most global ocean models or any global-coupled models, limiting their ability to accurately represent shelf seas, including the seasonal evolution of SST (J. Holt et al., 2017).

On regional scales, eddy-resolving ocean models forced with the main tidal constituents can simulate the observed stratification structure (e.g., AMM15; Graham et al., 2018) and are routinely applied to provide useful operational ocean forecasts (e.g., Tonani et al., 2019). Tides are included through both open boundary conditions and as a surface potential forcing in the ocean equations of motion. It is therefore feasible to remove tides in these models to isolate their impact and assess their role in the seasonal evolution of ocean stratification.

Coupled models provide an approach to explicitly simulate the feedback of any changes to the ocean surface on the overlying atmosphere without any relaxations in the seasonal evolution of regional SST (e.g.,

Kelemen et al., 2019; Wang et al., 2015). While several studies have demonstrated considerable sensitivity of the marine boundary layer to regional-scale SST variability (e.g., Fallmann et al., 2017; Frenger et al., 2013; Small et al., 2008), and how changes to SST impact precipitation over land (Kelemen et al., 2019; Lebeaupin Brossier et al., 2015), to the best of our knowledge, the impact of ocean tides on the weather has not been directly assessed and is therefore the focus of this paper. With this aim, a regional ocean–atmosphere–coupled system is used to run a summer and winter simulation with and without tides.

## 2. Modeling and Methods

### 2.1. Regional Modeling Experiments

For coupled simulations, the UKC4 regional-coupled prediction system was run in atmosphere–ocean–coupled mode with and without application of tidal forcing in the ocean component to assess the impact of tides on the British weather. Details of the model configuration and coupling approach are described in detail by Lewis et al. (2019), with only key aspects summarized below. All simulations are free running without data assimilation.

The ocean component of UKC4 uses the NEMO model code (Madec, 2016; vn3.6 revision 6232) set-up with the AMM15 (Atlantic Margin Model, 1.5 km) eddy-resolving shelf seas science configuration and related surface and lateral boundary forcing (Graham et al., 2018; Tonani et al., 2019). The tidal potential is calculated for 11 harmonic constituents over the domain. Tidal forcing is also applied along the lateral boundaries. The amplitude and phase for each of the constituents are defined at a resolution of  $1/12^\circ$  (TPXO7.2, Atlantic Ocean 2011-ATLA; Egbert & Erofeeva, 2002). Lateral ocean boundaries were provided by a  $1/12^\circ$  North Atlantic deep ocean NEMO configuration and climatological river discharge fluxes were applied (Tonani et al., 2019).

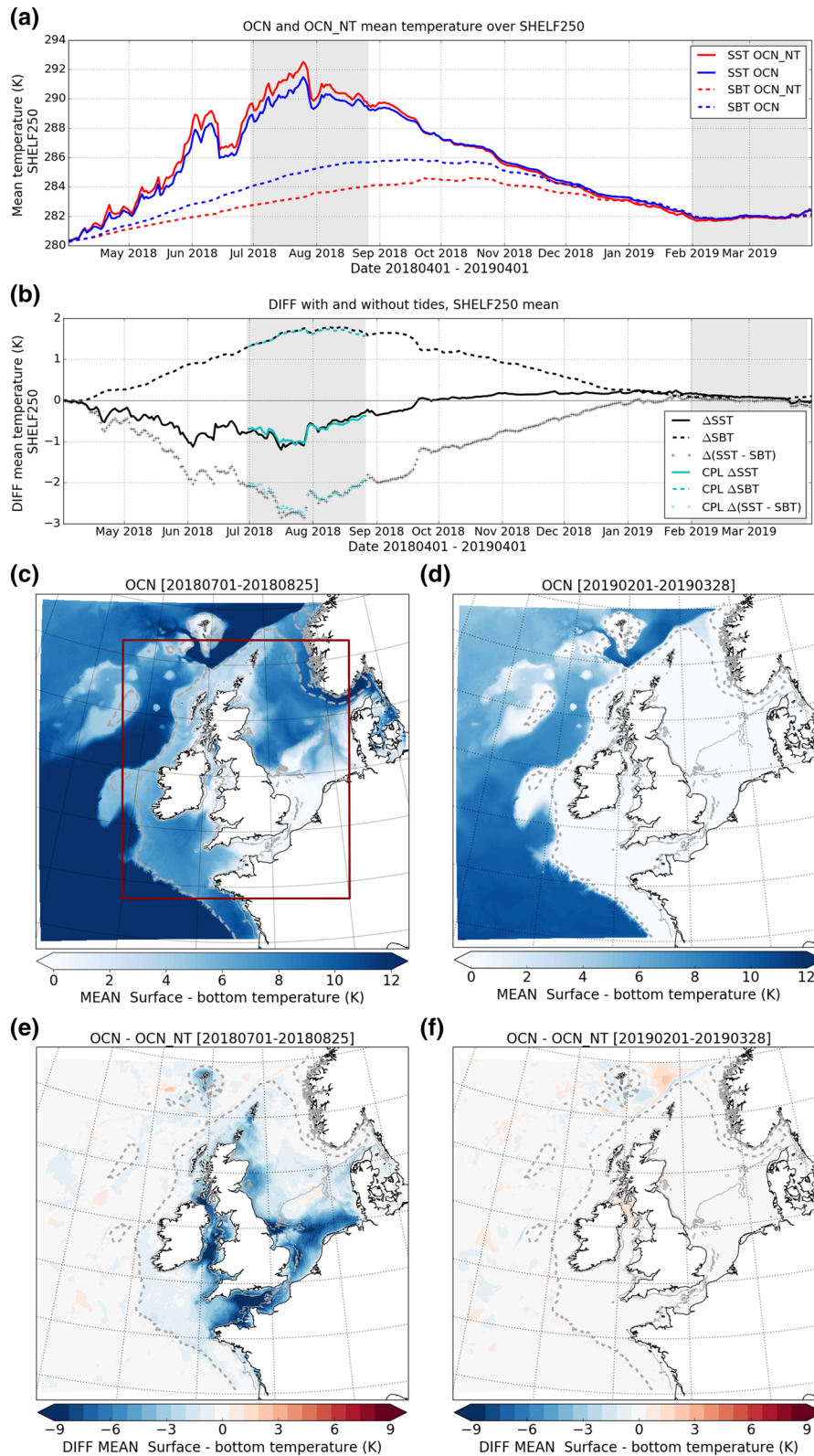
Simulated SST and surface currents from the ocean component are coupled hourly to an atmosphere model, using OASIS3-MCT libraries (Craig et al., 2017). UKC4 uses the Unified Model (UM; vn11.1) atmosphere and JULES land-surface model (Best et al., 2011), using the RAL1 science configuration (Bush et al., 2020). Turbulent fluxes of heat, moisture, and momentum over land and sea surfaces are calculated within JULES, using surface layer similarity theory (Bush et al., 2020), with SST and ocean currents used as evolving surface conditions in coupled simulations (Lewis et al., 2018). Initial atmosphere conditions were provided by operational Met Office regional analyses at the beginning of both test periods. Hourly lateral boundaries are derived from the first 24 h of operational global-scale NWP forecasts each day through the period, running at order 10-km resolution (Walters et al., 2019).

Both ocean and atmosphere model grids are centered on the United Kingdom (UK) and NWS and defined with grid spacing of 1.5 km in rotated polar coordinates (Lewis et al., 2019; see also Figure 1). The ocean grid has 51 vertical levels using stretched terrain-following coordinates, with the upper grid level set no more than 1 m below the surface. The atmosphere grid has 70 terrain-following vertical levels, with the lowest level set at 2.5 m above the surface.

Uncoupled ocean-only experiments were run with and without tides, termed OCN and OCN\_NT, respectively, for a year beginning April 1, 2018. The UKC4-coupled system was run for an 8-week simulation during summer 2018 (initialized on June 30, 2018) and another in winter 2019 (initialized on February 1, 2019) in order to assess the influence of tides at different stages of seasonal stratification (see areas shaded in gray in Figures 1(a) and 1(b)). Initial conditions for the ocean component of UKC4 for summer and winter periods were obtained from the ocean-only OCN and OCN\_NT simulations, respectively (see Section 2.2). The coupled simulations with tidal forcing applied in the NEMO ocean component are termed CPL and simulations without tides termed CPL\_NT.

### 2.2. Spin-Up of Tidal and Nontidal Ocean Conditions

Ocean-only simulations OCN and OCN\_NT were initialized from the same operational AMM15 restart. Global-scale operational meteorological forcing is applied using the flux forcing approach to be consistent with the coupled model exchanges. In spring, the impact of tides on the ocean state is relatively small and by summer 2018 the relative difference between OCN and OCN\_NT is well spun up (Figure 1(a)).



Figures 1(c) and 1(d) show the mean difference between simulated surface temperature and seabed temperature (SBT) when tides are included over 8 weeks during summer and winter. These panels highlight the well-studied strong seasonal contrast on the NWS in depths shallower than 250 m, with strong summer stratification but without winter stratification (e.g., Elliott & Clarke, 1991). The influence of tides on stratification (summarized as SST – SBT) is shown by OCN-OCN\_NT differences in Figures 1(e) and 1(f). Differences in stratification of over 8 K are found between OCN and OCN\_NT in summer through the shallow regions of the southern North Sea, English Channel, and Irish Sea, associated with tidal mixing fronts (e.g., J. T. Holt & Umlauf, 2008). Without tidal mixing, stratification develops more quickly in OCN\_NT as the warmth from radiative heating becomes trapped near the surface, resulting in both increasing the SST and decreasing the SBT relative to OCN results (Figure 1(b)). For both OCN and OCN\_NT, this gives rise to a maximum in stratification in July, although the difference in SST continues to increase until late summer (Figure 1(b)). In summer, the effect of tides on SBT is larger than on SST, and the seasonal evolution of SBT differences lags SST by several months (Figure 1(b)).

By February (Figures 1(d) and 1(f)), the NWS in both simulations is well mixed (hence very little stratification in either simulation) and there are much smaller differences in the temperature at the surface or at the seabed. This is expected since in winter, surface cooling in combination with tidal and wind mixing acts together to break down stratification. As a result of this, only small persisted impacts of the differences in stratification from the end of summer remain between the OCN and OCN\_NT simulations. Although the late winter differences in water column temperature are small, it remains to be seen whether the differences introduced by including tides could accumulate for simulations run over a number of years. This is not investigated here but may be relevant for climate studies (Lee et al., 2006).

### 3. Results: Impact of Ocean Stratification Changes on the Ocean and the Atmosphere

#### 3.1. Ocean Model Sensitivity to Tidal Forcing

Figure 2 shows the impact of tides on SST as monthly mean differences (OCN – OCN\_NT) for June–October 2018 and February 2019 for the region on the shelf outlined in the red box in Figure 1(c), where tides have most impact on stratification. The region within the red box in Figure 1(c), where the bathymetry is shallower than 250 m, will be referred to as SHELF250.

In summer, tidal mixing in OCN leads to widespread cooler SSTs on the shelf (Figure 2). The largest monthly SHELF250-mean difference of 0.9 K was found in July, with local differences of up to 8 K. A widespread pattern of SBT warming in OCN compared to OCN\_NT in the shelf region develops and peaks in August (Figure 1(b)), where the monthly SHELF250-mean difference is 1.7 K (with values reaching 9.7 K).

Also apparent in Figure 2 is the decreasing impact of tides on SST through autumn months. By October 2018 (Figure 2(e)), the monthly SHELF250-mean temperature difference between OCN and OCN\_NT is 0.1 K, with differences ranging within  $\pm 2$  K. When tides are included, the cooler summer SST results in reductions in SST-dependent upwards turbulent and longwave fluxes, as well as increased downward heat transport due to tidal mixing all of which warm the subsurface ocean and lead to increased heat storage when tides are included. At the end of the summer, convection, tide, and wind-driven vertical mixing causes this warm subsurface signal to reemerge at the surface.

By midwinter, the magnitude of the mean tidal SST differences has reduced further at most locations—although the monthly SHELF250-mean difference for February 2019 is also 0.1 K. The slight winter warming

---

**Figure 1.** (a) Time series of mean sea-surface (SST) and seabed (SBT) temperature for OCN and OCN\_NT simulations over a year, beginning April 2018, for all regions in the red box shown in (c) where the bathymetry is shallower than 250 m, termed “SHELF250.” (b) Time series for SHELF250 showing differences between OCN and OCN\_NT in mean SST and SBT. Differences between CPL and CPL\_NT shown for summer period. (c) Two-month (8-week) mean difference between simulated SST and SBT, indicative of the vertical stratification, in the OCN simulation during July–August 2018 (summer). Plot (d) is as in (c) but for February–March 2019 (winter). (e, f) Mean difference in stratification between OCN and OCN\_NT simulations in summer and winter, respectively. The dashed and solid gray contour lines mark areas where the bathymetry is 250 m and 50 m or shallower, respectively.

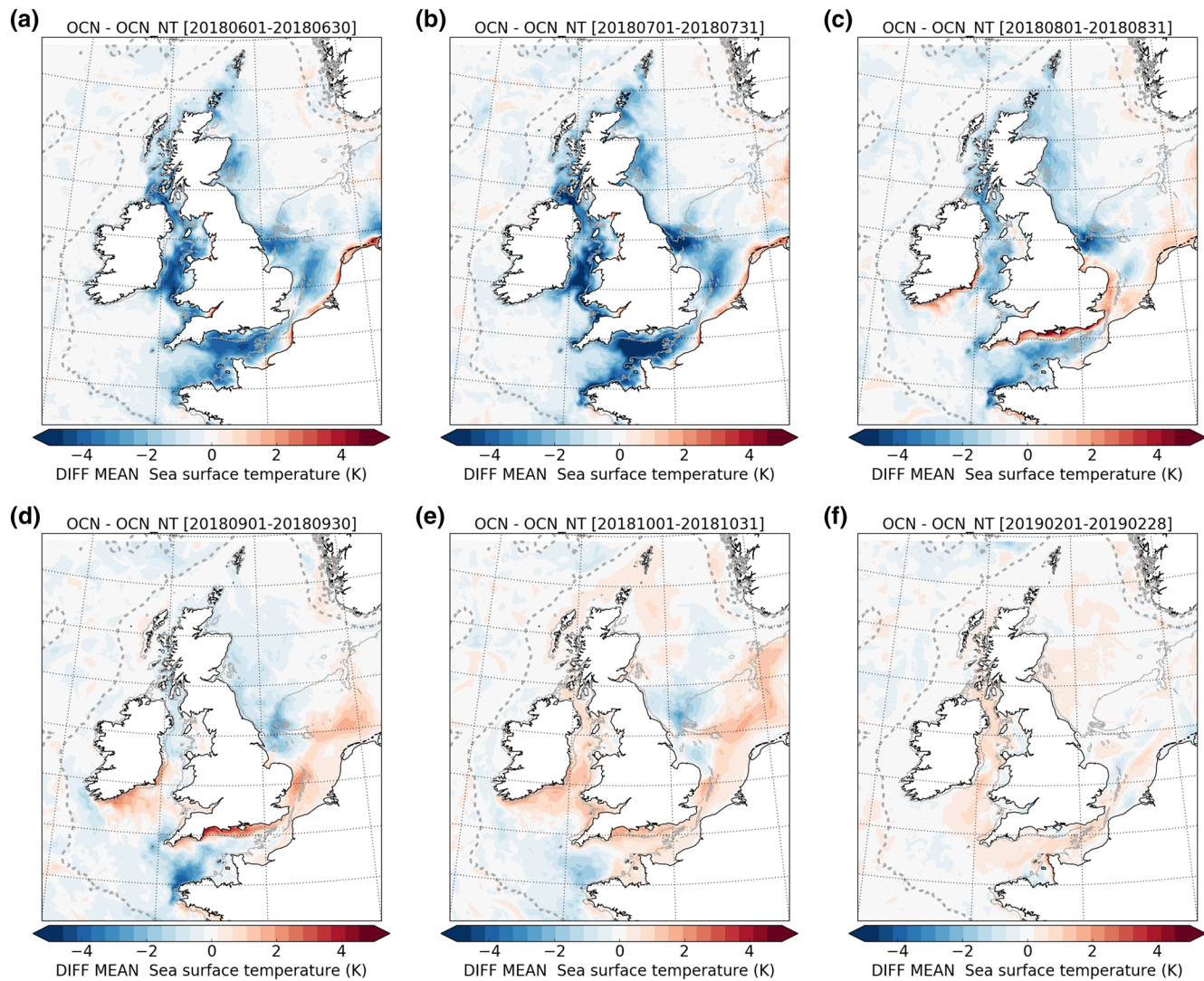


**Figure 2.** Monthly mean SST differences between OCN and OCN\_NT during (a) June, (b) July, (c) August, (d) September, and (e) October 2018 and (f) February 2019. The region shown is the subdomain indicated by the red box in Figure 1(c). The dashed and solid gray contour lines mark areas where the bathymetry is 250 m and 50 m or shallower, respectively. SST, sea-surface temperature.

is particularly focused in those areas with the coolest summer surface temperatures, when tides are included (Figure 2) and is therefore attributed to the impact of increased summer heat storage as a result of tidal mixing.

As both SST and currents are coupled to the atmosphere in UKC4, the impacts of tidal forcing on surface current speeds were also assessed (plots not shown). Surface residual current speeds are decreased by about 20% of the simulated SHELF250-mean speed, with the inclusion of tides in both summer and winter periods.

### 3.2. Impact of Ocean Tides on the Marine Boundary Layer

The sensitivity of the near-surface atmosphere to tides is assessed by comparing CPL and CPL\_NT simulations over the 8-week periods in July–August 2018 and February–March 2019. This analysis focuses on the summer when the influence of tidal forcing on the ocean is largest. Figure 3 shows the period-mean influence of tides on simulated surface temperature ( $T_{sfc}$ ), 1.5 m air temperature ( $T_{air}$ ), and 10 m wind speed ( $U_{10}$ ) for the same subregion presented in Figure 2 (see red box in Figure 1(c)). Time series of the area-mean

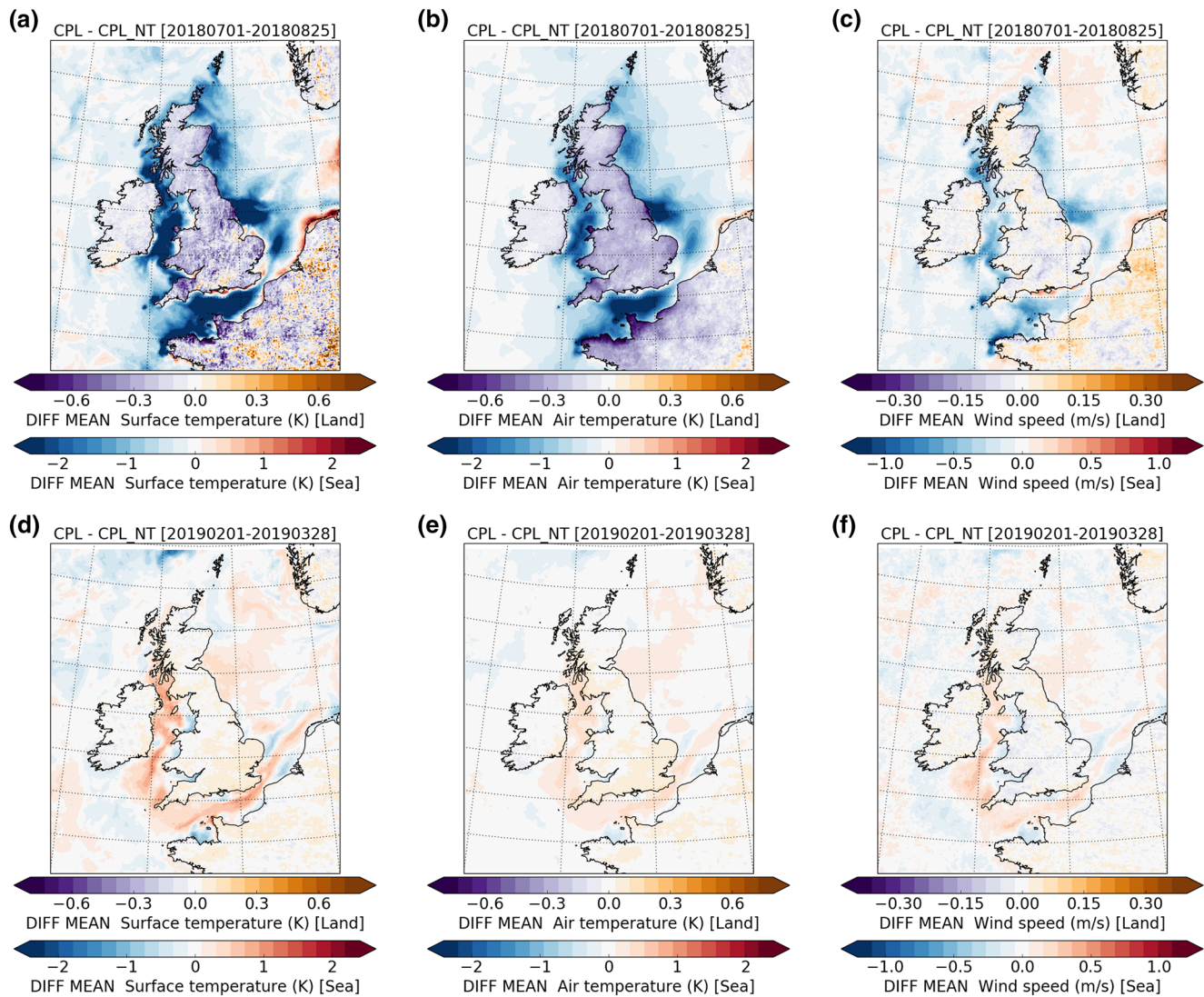


**Figure 3.** Two-month (8-week) mean differences between CPL and CPL\_NT simulations of (a) surface temperature ( $T_{\text{sfc}}$ ), (b) 1.5 m air temperature ( $T_{\text{air}}$ ), and (c) 10 m wind speed ( $U_{10}$ ) in summer 2018. (d–f) The corresponding differences in winter 2019. Note different color scales are used to highlight land and sea differences separately. The region shown is the subdomain indicated by the red box in Figure 1(c).

differences during these periods are presented in Figure 4, separately for SHELF250 sea points and land (GB only) points.

The coupled model  $T_{\text{sfc}}$  differences (CPL – CPL\_NT) over the ocean in Figure 3 are consistent with the ocean-only SST differences (OCN – OCN\_NT) in Figure 2, as expected. The mean difference in  $T_{\text{sfc}}$  over the 8-week summer period across SHELF250 was a cooling of 0.8 K in CPL relative to CPL\_NT and up to 5.5 K cooler locally (Figure 3(a)). The corresponding mean SST difference in the uncoupled model (OCN – OCN\_NT) was slightly less (0.7 K) over the same period but with larger extremes, reaching 6.4 K cooler locally. The differences in SST, SBT, and stratification in the coupled model closely match those in the uncoupled model (Figure 1(b)).

Changes in SST directly translate into differences in the sensible, latent, and longwave heat fluxes, as they all depend on  $T_{\text{sfc}}$ . This alters the state of the overlying atmosphere, particularly the boundary layer height and characteristics, which then feed back onto all the flux components including short wave in an iterative adjustment process. Over the ocean in summer (not shown), large reductions in upwards sensible (SHELF250-mean difference  $1.9 \text{ W m}^{-2}$ ) and latent (SHELF250-mean difference  $10.8 \text{ W m}^{-2}$ ) heat flux are evident over

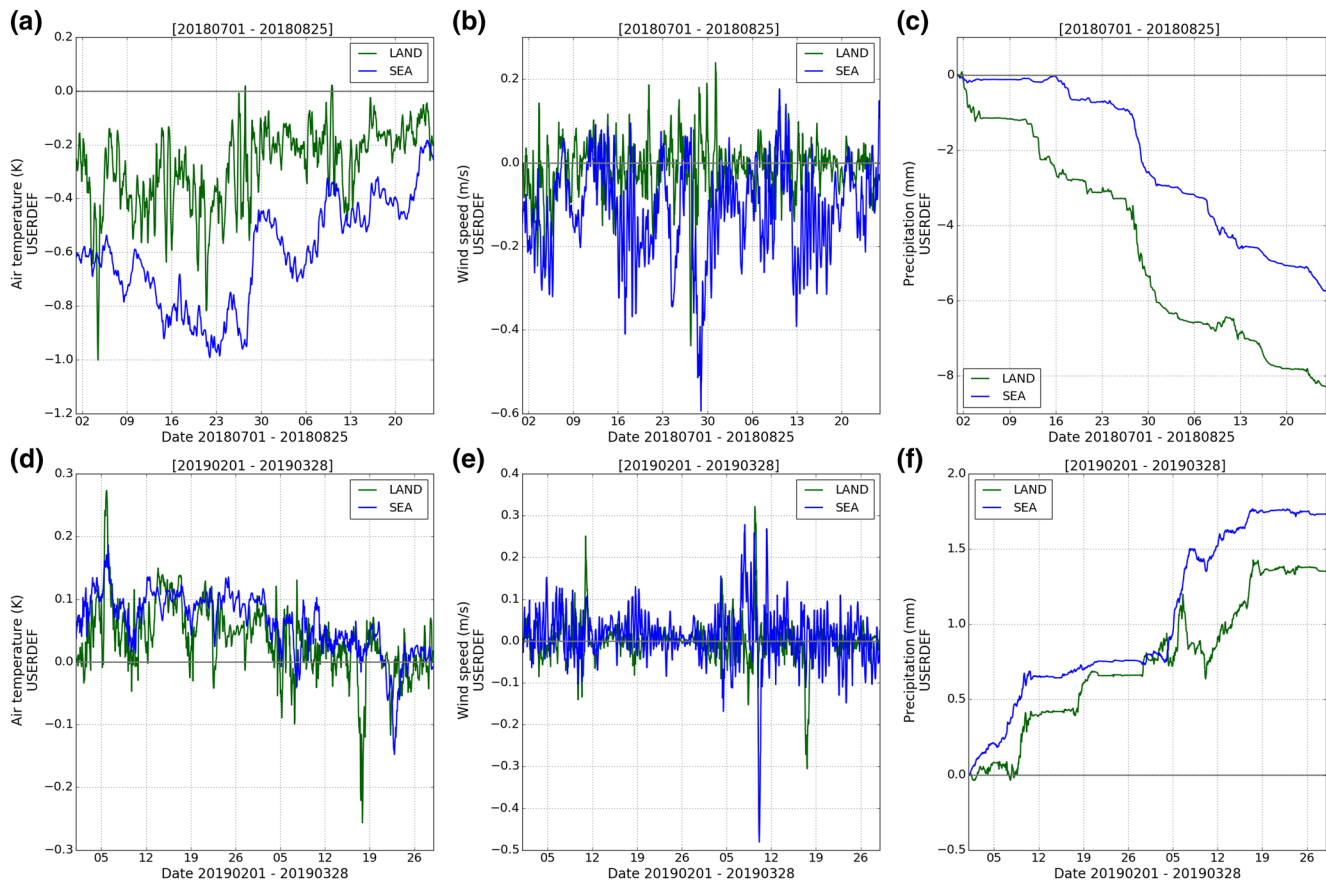


**Figure 4.** Time series of region-mean differences CPL – CPL\_NT of (a, d) 1.5 m air temperature, (b, e) 10 m wind speed, and (c, f) accumulated precipitation during summer (top) and winter (bottom) simulations, respectively, computed for the subregion shown in Figure 3. “SEA” label indicates SHEL250 area and “LAND” label indicates Great Britain. Accumulated precipitation differences are shown as a cumulative mean precipitation difference for clarity.

the cooler SSTs when tides are included. The net impact of these flux differences on the near-surface  $T_{\text{air}}$  is shown in Figure 3(b). Over the summer period, the SHEL250-mean difference in  $T_{\text{air}}$  (CPL – CPL\_NT) over the ocean is 0.6 K cooler (up to 3 K cooler locally). The relative magnitudes of  $T_{\text{air}}$  adjustment and local SST differences are consistent with the results of Petch et al. (2020), who forced a UM regional configuration with widespread SST anomaly perturbations of 3 K for a summer heatwave case. When comparing model output to observations (not shown), the bias in CPL for  $T_{\text{air}}$  over the 8-week summer period of 0.1 is notably smaller than the CPL\_NT bias of 0.87.

For the winter period, the SHEL250-mean SST (CPL–CPL\_NT) difference is 0.08 K, and local time-mean differences are within  $\pm 2.5$  K. This results in more limited adjustments of the near-surface flux components and leads to a mean  $T_{\text{air}}$  warming over SHEL250 of 0.06 K, with local differences between  $-1.1$  K and  $+0.7$  K. Over the winter period, CPL has a bias of 0.25 when comparing to  $T_{\text{air}}$  observations, larger than the bias in CPL\_NT of 0.14.

In both summer and winter, there is a clear imprint of  $T_{\text{sfc}}$  and  $T_{\text{air}}$  differences on the pattern of near-surface wind speed differences due to tides (Figures 3(c) and 3(f)). As highlighted by Lewis et al. (2019; see their Figure 14), this is driven by the changes in near-surface stability. Where there are warmer SSTs, the overlying atmosphere is less stable leading to a deeper and more turbulent boundary layer. As a result, the vertical wind shear relative to winds aloft is reduced, driving faster wind speeds at 10 m. A similar relationship between near-surface stability and wind speed changes is found for this study (not shown) and suggests that surface current changes do not play a large role in impacting wind speed.

### 3.3. Impact of Ocean Tides on the Weather Over Land

It was expected that differences in SST induced by including tides would cause local changes in near-surface fluxes and temperatures, stability, and wind speed over the ocean; however, the primary interest in this study is the sensitivity of weather over land areas to the tides.

The main feature highlighted by Figures 3(b) and 4(a) is a consistent and widespread cooling of mean  $T_{\text{air}}$  over land areas in summer when tides are included. Considering only the GB land area (Scotland, England, and Wales), including tides, leads to an 8-week area-mean reduction in  $T_{\text{air}}$  of 0.3 K, with local differences of up to 1.4 K cooler. The largest sensitivity to tides is found in near-coastal regions of Wales, South-West England, and East Anglia, although nearly all GB land grid points show a cooling due to tides. This is likely to be due to the advection of relatively cooler air from over the ocean with tides, driven both by prevailing winds and by sea breezes. There are also contributions resulting from tidally driven changes in these atmospheric circulations—illustrated by highly complex and variable differences in  $T_{\text{air}}$  over land for any particular location and point in time.

As shown in Figure 3(c), including tides also affects wind speed over land (more so in summer than in winter); however, there is much greater spatial variability in the impact of tides on mean  $U_{10}$  than for  $T_{\text{air}}$ , with no clear resulting change in the mean wind speed over the GB land region as a whole (Figures 3(c) and 4(b)).

While the impact of tides on the SST and  $T_{\text{air}}$  over the ocean is smaller in winter, the mean differences over land and sea points are comparable. The 8-week mean difference in  $T_{\text{air}}$  over GB land areas is 0.04 K warmer with tides and within  $\pm 0.2$  K (largest differences focused in Southern England). The SHEL250-mean is 0.06 and the range of local mean differences is larger over the ocean, varying between  $-1.1$  K and 0.7 K.

The net impact of ocean tides on precipitation over sea and land areas is shown in Figures 4(c) and 4(f) as the cumulative difference in precipitation between CPL and CPL\_NT simulations. In summer over GB land areas, the 8-week accumulated precipitation is over 8 mm less when tides are included. This is 6% of the total accumulated precipitation over land in the nontidal run (of 134 mm) for that period. The SHEL250 difference in accumulated precipitation over the ocean when including tides is the same (6% of the total over the ocean, the total in the nontidal run being 100 mm). In winter, the total accumulated precipitation in the nontidal run was 186 mm and 160 mm over GB land and SHEL250 sea, respectively. Including tides increased the amount of precipitation, more so over the ocean than over land, though only marginally. The differences were 1.5 mm (0.8%) over land and 1.8 mm (1%) over sea regions. This could be expected as the tidal SST and marine air temperature and humidity differences are much smaller in winter.

This result is consistent with the anticipated response of relatively cooler air being able to hold less precipitable water (e.g., Dado & Takahashi, 2017; Kendon et al., 2014) in summer and the slight increase in winter, consistent with a relative warming over land when tides are included.

## 4. Discussion and Conclusions

This study illustrates the sensitivity of the British weather, particularly during summer, to the strong tides that propagate around its coastal waters. During spring and summer when surface heating is strong, tidal mixing reduces stratification and increases vertical heat transport compared to equivalent simulations without tides. In some shallow and tidally energetic regions, tidal mixing prevents stratification from developing so waters remain mixed, whereas without tides they become stratified. Consequently, in these regions, including tides generally leads to cooler surface temperatures and warmer seabed temperatures relative to simulations without tides.

By making novel use of a regional atmosphere–ocean-coupled modeling system, it has been possible to quantify the influence of SST changes both locally on the marine boundary layer temperature, wind speed, and precipitation and the extent to which these impacts propagate inland.

Some clear signals emerge. During the summer period, a mean SST decrease with tidal mixing of 0.7 K, decreases the mean near-surface air temperatures over the sea by 0.6 K. Over GB land areas, the mean air

temperature is 0.3 K cooler with tides. Relatively small but consistent decreases in wind speed and an increased accumulated precipitation of 6% of the summer total are also evident over land areas. By contrast in winter, due to the reemergence of the summer warm subsurface signal, an SST increase of 0.08 K with tides is evident and results in a smaller sensitivity of British weather to tides. Tidally driven air temperature differences over land are found to be typically about 10% the magnitude but of the opposite sign to those in summer.

Global and regional-scale climate simulations (e.g., Kendon et al., 2014; Roberts et al., 2019) are typically either directly or indirectly driven by global-scale analyses and model projections which do not include regional-scale processes such as tides (e.g., J. Holt et al., 2017; Timko et al., 2019). These results therefore have considerable implications for the fidelity of regional projections and highlight seasonal changes in the likely impact of missing tidal processes, with the largest impact in summer. Application of regional-coupled prediction systems including tides and other small-scale atmospheric and ocean processes at km-scale (e.g., Gutowski et al., 2020; Hermans et al., 2020; Kelemen et al., 2019) should provide more robust projections for future changes for near-coastal marine and land regions.

It should be noted that 2018 was an exceptionally warm summer which has possibly accentuated the differences between the run with tide compared to without tides. However, these summer extremes are considered to be more likely in a changing climate (Christidis et al., 2020; Molina et al., 2020; Schoetter et al., 2015), so this study is likely to remain relevant to the sensitivity of British weather to ocean tides in coming decades. This information is of increasing importance both to provide climate services and for regional-scale adaptation policy.

### Conflict of Interest

The authors share no conflict of interest.

### Data Availability Statement

The source code for the model used in this study is available to use. NEMO codes are available after registration at <http://www.nemo-ocean.eu>, and a license for the UM code can be applied for here: <http://www.metoffice.gov.uk/research/collaboration/um-collaboration>. Data used to produce the figures are available from <https://doi.org/10.5281/zenodo.4302340>.

### Acknowledgments

This research has been carried out under national capability funding as part of UK Environmental Prediction, in collaboration between the Met Office, Centre for Ecology and Hydrology (CEH), National Oceanography Center (NOC), and Plymouth Marine Laboratory (PML). The authors would particularly like to thank the reviewers for their extensive work and valuable comments. This work was also supported by the Met Office Hadley Centre Climate Programme funded by BEIS and Defra.

### References

- Best, M. J., Pryor, M., Clark, D. B., Rooney, G. G., Essery, R. L. H., Ménard, C. B., et al. (2011). The Joint UK Land Environment Simulator (JULES), model description—Part 1: Energy and water fluxes. *Geoscientific Model Development*, 4, 677–699. <https://doi.org/10.5194/gmd-4-677-2011>
- Bowers, D. G., & Roberts, E. M. (2019). *Tides: A very short introduction*. Oxford, UK: Oxford University Press.
- Bush, M., Allen, T., Bain, C., Boutle, I., Edwards, J., Finnenkoetter, A., et al. (2020). The first Met Office Unified Model/JULES Regional Atmosphere and Land configuration, RAL1. *Geoscientific Model Development*, 13, 1999–2029. <https://doi.org/10.5194/gmd-13-1999-2020>
- Christidis, N., McCarthy, M., & Stott, P. A. (2020). The increasing likelihood of temperatures above 30 to 40 °C in the United Kingdom. *Nature Communications*, 11, 3093. <https://doi.org/10.1038/s41467-020-16834-0>
- Craig, A., Valcke, S., & Coquart, L. (2017). Development and performance of a new version of the OASIS coupler, OASIS3-MCT\_3.0. *Geoscientific Model Development*, 10, 3297–3308. <https://doi.org/10.5194/gmd-10-3297-2017>
- Dado, J. M. B., & Takahashi, H. G. (2017). Potential impact of sea surface temperature on rainfall over the western Philippines. *Progress in Earth and Planetary Science*, 4, 23. <https://doi.org/10.1186/s40645-017-0137-6>
- Egbert, G. D., & Erofeeva, S. Y. (2002). Efficient inverse modeling of barotropic ocean tides. *Journal of Atmospheric and Oceanic Technology*, 19(2), 183–204. [https://doi.org/10.1175/1520-0426\(2002\)019<0183:EIMOB0>2.0.CO;2](https://doi.org/10.1175/1520-0426(2002)019<0183:EIMOB0>2.0.CO;2)
- Elliott, A. J., & Clarke, T. (1991). Seasonal stratification in the northwest European shelf seas. *Continental Shelf Research*, 11(5), 467–492. [https://doi.org/10.1016/0278-4343\(91\)90054-A](https://doi.org/10.1016/0278-4343(91)90054-A)
- Fallmann, J., Lewis, H., Castillo, J. M., Arnold, A., & Ramsdale, S. (2017). Impact of sea surface temperature on stratiform cloud formation over the North Sea. *Geophysical Research Letters*, 44, 4296–4303. <https://doi.org/10.1002/2017GL073105>
- Frenger, I., Gruber, N., Knutti, R., & Münnich, M. (2013). Imprint of Southern Ocean eddies on winds, clouds and rainfall. *Nature Geoscience*, 6, 608–612. <https://doi.org/10.1038/ngeo1863>
- Graham, J. A., O’Dea, E., Holt, J., Polton, J., Hewitt, H. T., Furner, R., et al. (2018). AMM15: A new high-resolution NEMO configuration for operational simulation of the European north-west shelf. *Geoscientific Model Development*, 11, 681–696. <https://doi.org/10.5194/gmd-11-681-2018>

- Gutowski, W. J., Jr., Ullrich, P. A., Hall, A., Leung, L. R., O'Brien, T. A., Patricola, C. M., et al. (2020). The ongoing need for high-resolution regional climate models: Process understanding and stakeholder information. *Bulletin of the American Meteorological Society*, 101(5), E664–E683. <https://doi.org/10.1175/BAMS-D-19-0113.1>
- Hermans, T. H. J., Tinker, J., Palmer, M. D., Katsman, C. A., Vermeersen, B. L. A., & Slangen, A. B. A. (2020). Improving sea-level projections on the Northwestern European shelf using dynamical downscaling. *Climate Dynamics*, 54, 1987–2011. <https://doi.org/10.1007/s00382-019-05104-5>
- Holt, J., Hyder, P., Ashworth, M., Harle, J., Hewitt, H. T., Liu, H., et al. (2017). Prospects for improving the representation of coastal and shelf seas in global ocean models. *Geoscientific Model Development*, 10, 499–523. <https://doi.org/10.5194/gmd-10-499-2017>
- Holt, J. T., & Umlauf, L. (2008). Modeling the tidal mixing fronts and seasonal stratification of the Northwest European Continental shelf. *Continental Shelf Research*, 28(7), 887–903. <https://doi.org/10.1016/j.csr.2008.01.012>
- Kelemen, F. D., Primo, C., Feldmann, H., & Ahrens, B. (2019). Added value of atmosphere–ocean coupling in a century-long regional climate simulation. *Atmosphere*, 10, 537. <https://doi.org/10.3390/atmos10090537>
- Kendon, E., Roberts, N., Fowler, H., Roberts, M. J., Chan, S. C., & Senior, C. A. (2014). Heavier summer downpours with climate change revealed by weather forecast resolution model. *Nature Climate Change*, 4, 570–576. <https://doi.org/10.1038/nclimate2258>
- Lebeauupin Brossier, C., Bastin, S., Béranger, K., & Drobinski, P. (2015). Regional mesoscale air–sea coupling impacts and extreme meteorological events role on the Mediterranean Sea water budget. *Climate Dynamics*, 44, 1029. <https://doi.org/10.1007/s00382-014-2252-z>
- Lee, H.-C., Rosati, A., & Spelman, M. J. (2006). Barotropic tidal mixing effects in a coupled climate model: Oceanic conditions in the northern Atlantic. *Ocean Modelling*, 11, 464–477. <https://doi.org/10.1016/j.ocemod.2005.03.003>
- Lewis, H. W., Castillo Sanchez, J. M., Arnold, A., Fallmann, J., Saulter, A., Graham, J., et al. (2019). The UKC3 regional coupled environmental prediction system. *Geoscientific Model Development*, 12, 2357–2400. <https://doi.org/10.5194/gmd-12-2357-2019>
- Lewis, H. W., Castillo Sanchez, J. M., Graham, J., Saulter, A., Bornemann, J., Arnold, A., et al. (2018). The UKC2 regional coupled environmental prediction system. *Geoscientific Model Development*, 11, 1–42. <https://doi.org/10.5194/gmd-11-1-2018>
- Madec, G. (2016). *NEMO reference manual 3.6\_STABLE: "NEMO ocean engine" Note du Pôle de modélisation* (No. 27). France: Institut Pierre-Simon Laplace (IPSL). <https://doi.org/10.5281/zenodo.3248739>
- Molina, M. O., Sánchez, E., & Gutiérrez, C. (2020). Future heat waves over the Mediterranean from an Euro-CORDEX regional climate model ensemble. *Scientific Reports*, 10, 8801. <https://doi.org/10.1038/s41598-020-65663-0>
- Nauw, J., Haas, H., & Rehder, G. (2015). A review of oceanographic and meteorological controls on the North Sea circulation and hydrodynamics with a view to the fate of North Sea methane from well site 22/4b and other seabed sources. *Marine and Petroleum Geology*, 68, 861–882. <https://doi.org/10.1016/j.marpetgeo.2015.08.007>
- Petch, J. C., Short, C. J., Best, M. J., McCarthy, M., Lewis, H. W., Vosper, S. B., & Weeks, M. (2020). Sensitivity of the 2018 UK summer heatwave to local sea temperatures and soil moisture. *Atmospheric Science Letters*, 21, e948. <https://doi.org/10.1002/asl.948>
- Roberts, M. J., Baker, A., Blockley, E. W., Calvert, D., Coward, A., Hewitt, H. T., et al. (2019). Description of the resolution hierarchy of the global coupled HadGEM3-GC3.1 model as used in CMIP6 HighResMIP experiments. *Geoscientific Model Development*, 12, 4999–5028. <https://doi.org/10.5194/gmd-12-4999-2019>
- Schoetter, R., Cattiaux, J., & Douville, H. (2015). Changes of western European heat wave characteristics projected by the CMIP5 ensemble. *Climate Dynamics*, 45, 1601–1616. <https://doi.org/10.1007/s00382-014-2434-8>
- Simpson, J. H., Allen, C. M., & Morris, N. C. G. (1978). Fronts on the continental shelf. *Journal of Geophysical Research*, 83, 4607–4614.
- Simpson, J. H., & Hunter, J. R. (1974). Fronts in the Irish Sea. *Nature*, 250, 404–406. <https://doi.org/10.1038/250404a0>
- Small, R. J., Xie, S. P., O'Neill, L., Seo, H., Song, Q., Cornillon, P., et al. (2008). Air–sea interaction over ocean fronts and eddies. *Dynamics of Atmospheres and Oceans*, 45(3–4), 274–319. <https://doi.org/10.1016/j.dynatmoce.2008.01.001>
- Timko, P. G., Arbic, B. K., Hyder, P., Richman, J. G., Zamudio, L., O'Dea, E., et al. (2019). Assessment of shelf sea tides and tidal mixing fronts in a global ocean model. *Ocean Modelling*, 136, 66–84. <https://doi.org/10.1016/j.ocemod.2019.02.008>
- Tonani, M., Sykes, P., King, R. R., McConnell, N., Péquignat, A.-C., O'Dea, E., et al. (2019). The impact of a new high-resolution ocean model on the Met Office North-West European Shelf forecasting system. *Ocean Science*, 15, 1133–1158. <https://doi.org/10.5194/os-15-1133-2019>
- van Leeuwen, S., Tett, P., Mills, D., & van der Molen, J. (1995). Stratified and nonstratified areas in the North Sea: Long-term variability and biological and policy implications. *Journal of Geophysical Research: Oceans*, 120, 4670–4686. <https://doi.org/10.1002/2014JC010485>
- Walters, D., Baran, A. J., Boutle, I., Brooks, M., Earnshaw, P., Edwards, J., et al. (2019). The Met Office Unified Model Global Atmosphere 7.0/7.1 and JULES Global Land 7.0 configurations. *Geoscientific Model Development*, 12, 1909–1963. <https://doi.org/10.5194/gmd-12-1909-2019>
- Wang, S., Dieterich, C., Döscher, R., Höglund, A., Hordoir, R., Meier, M. H. E., et al. (2015). Development and evaluation of a new regional coupled atmosphere–ocean model in the North Sea and Baltic Sea. *Tellus A: Dynamic Meteorology and Oceanography*, 67(1), 24284. <https://doi.org/10.3402/tellusa.v67.24284>